Processing, Characterization and Mechanical Properties of SiAlONs Produced from Low Cost β-Si_3N_4 Powder†

Hasan Mandal[1]* **and Nurcan Calis Acikbas**[2]
[1] *Materials Science and Engineering Programme, Sabancı University*
[2] *Department of Mechanical and Manufacturing Engineering, Engineering Faculty, Bilecik S.E. University*

Abstract

SiAlON ceramics have been known for many years as prime candidate materials in structural applications at ambient and high temperatures involving superior mechanical and/or chemical processes. In spite of their excellent properties, the utilization of SiAlONs has remained limited till today due to the high cost of raw materials and processing. In order to circumvent this problem, low cost refractory grade, coarse, impure, less sinter active β-Si_3N_4 *powder was used to produce SiAlON ceramics with satisfactory mechanical properties.*

In this article, the processing challenges in the production of SiAlON ceramics with β-Si_3N_4 *powder were discussed. The process parameters obviously affect the phase assemblage, densification, microstructural and mechanical properties of final SiAlON ceramics. Processed* β-Si_3N_4 *powder characteristics are majorly investigated by SEM-EDX, XRD, XRF, laser particle sizer and elemental analyser. The existence of undesirable impurities in the* β*-SiAlON crystal structure because of the use of impure* Si_3N_4 *powders has been shown to be tolerable by TEM microstructural analysis. Mechanical properties are in general evaluated by Vickers indentation method. Wear behaviour of the cost effective SiAlONs were compared with commercially available ceramic materials which are commonly being used in wear applications. Initially the use of such powders to produce materials for engineering applications proved challenging, however, satisfactory results have been obtained by the optimization of the initial chemical composition and process parameters.*

Keywords: powder processing, β-Si_3N_4 powder, particle size, sintering, characterization, wear

1. Introduction

SiAlON ceramic materials are very significant with their highly desirable, and proved potential, especially in industrial wear and high temperature applications[1-3]. The final mechanical and chemical properties of these ceramics depend on microstructural evolution (grain size, grain aspect ratio, porosity, intergranular phase, impurities, etc.)[4-7]. Powder processing stage has a strong effect on microstructural development, since ceramic parts are produced by the sintering of initial powder mixtures[8-12]. Removal of impurities from the raw powders, initial particle size distribution, homogeneous dispersion of sintering additives, and grinding of starting non-oxide powders are the important parameters in the microstructural formation of SiAlON materials with superior mechanical properties[13-19]. SiAlON production processes are based on homogenization of raw powders α or β-Si_3N_4 powder, Al_2O_3, AlN and sintering additives such as Y_2O_3, Sm_2O_3, Er_2O_3, Dy_2O_3, CaO, etc. in alcohol or water in order to achieve a predetermined composition (α:β-SiAlON ratio (α':β'), a determined intergranular phase chemistry),

---

† Accepted:August 10, 2012

1 Orhanli, Tuzla/Istanbul, 34956 Turkey
2 Bilecik, 11210, Turkey
* Corresponding author:
E-mail: hmandal@sabanciuniv.edu
TEL: +90-216-4839666 FAX: +90-216-4839118

followed by drying of slurry, shaping, and sintering.

Traditionally, high quality pure α-Si_3N_4 powder is used instead of β-Si_3N_4 powder due to its higher sinter activity. However, fine α-Si_3N_4 powders are very high in cost and this is a key determinant parameter for large scale applications. On the other hand, β-Si_3N_4 powders can be produced economically with combustion synthesis[20]. Free silicon and iron may originate from milling of the raw β-Si_3N_4 powder. Removal of these impurities and/or achieving desired final phases including these impurities in the sintered product is required. Besides milling and sintering process parameters have crucial effects on microstructural evolution. In this respect, SiAlON powder processing technology involves a number of know-how developments to produce materials with superior properties at low cost.

In this article, the manufacture low cost SiAlON ceramics with satisfactory mechanical properties by the use of low cost refractory grade, impure, less sinter active β-Si_3N_4 powder was described. Correlation between processed β-Si_3N_4 powder characteristics and process conditions with final phase assemblage, densification, microstructure and mechanical properties was determined.

2. Experimental Studies

In this study β-Si_3N_4 powder manufactured by combustion synthesis (Beijing Chanlian-Dacheng Trade Co. Ltd., China) was used as initial Si_3N_4 powder. Attrition milling in water with Si_3N_4 grinding media (3 mm in diameter) at 1400 rpm was performed to decrease the average particle size of β-Si_3N_4 starting powder. In order to completely understand correlation between processing-structure-property relationships, β-Si_3N_4 powder characteristics were investigated by using SEM-EDX, XRD, XRF, laser particle sizer and elemental analyser.

Since α' and β' phases are both stable thermodynamically, it is possible to produce hard and tough α-β-SiAlON composites. For this purpose $30\alpha:70\beta$-SiAlON composition was designed and Y-Sm-Ca multi cation doping system was chosen with the aim to produce self reinforcement microstructures. Y_2O_3 (>99.9%, H.C. Starck Berlin, Germany), Sm_2O_3 (>99.9%, Stanford Materials Corp., USA), $CaCO_3$ (>99.75%, Reidel-de Haen, Germany) were used as sintering additives. CaO was used to avoid α to β SiAlON transformation, Y_2O_3 and/or Re_2O_3 (where $Z_{Re} \geq 62$)) to increase the stability and hardness of α-SiAlON and Sm_2O_3 (where $Z_{Re} < 62$) to develop elongated β-SiAlON grains to increase fracture toughness). Si_3N_4 powders and sintering additives were mixed with high purity AlN powder (H Type, Tokuyama Corp. Japan, with 1.6wt% O content) and Al_2O_3 (Alcoa A16-SG Pittsburgh, USA). All of the prepared SiAlON compositions with β-Si_3N_4 powders were milled in water with 64wt% solid loadings. Tetramethylammonium hydroxide (TMAH) was used as a dispersant with 2.5 wt%. Milling was performed for a total duration of two hours. The slurry was sieved with 32 µm and homogenized together with 2 wt % plasticizer (Primal B60, Rhöm & Haas, Italy), 2 wt % binder (PEG 4000, Clariant Produkte GmbH, Germany) and 2 wt% lubricant (Zuzoplast Wem, ZSC Zimmer&Shwarz, Germany) in a mixer. The slurries were spray dried (Nubilosa LTC-2 model). The powders were uniaxially pressed at 25 MPa and subsequently cold isostatically pressed at 300 MPa to improve green density. Binder burn-out process was carried out at 550 ℃ for 30 minutes. The pellets were sintered both by gas pressure sintering (KCE, FPW 100/150-2200-25 type furnace), under 2.2 MPa nitrogen gas in a stan-

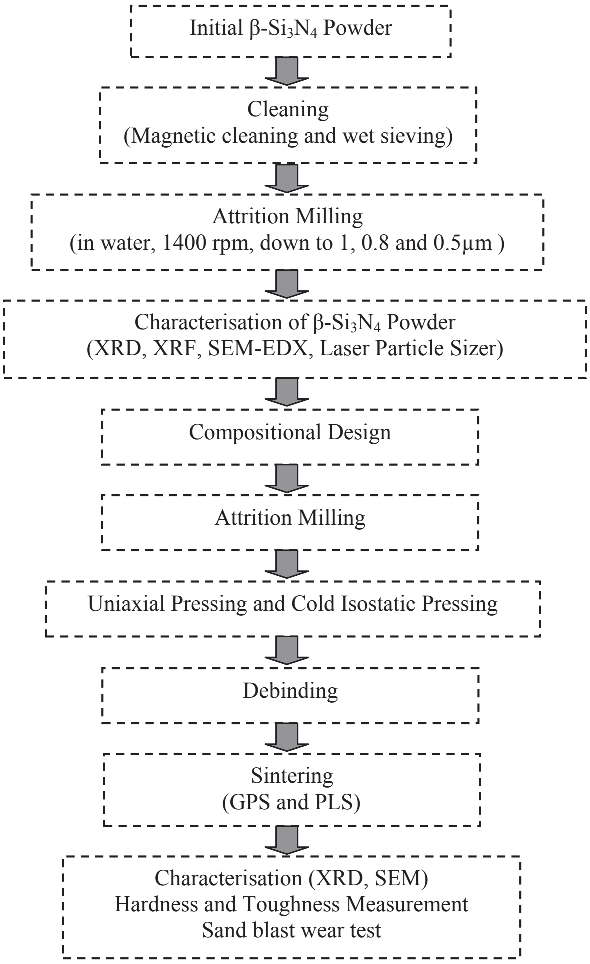

Fig. 1 Flow chart of the manufacturing process.

Table 1 Sand blast test conditions

Pressure	6 bar
Particle composition	Alumina
Particle size of alumina	0.5-1 mm
Alumina content	2 kg
Sample dimensions	24.5 × 7 mm
Test duration	10 min.
Distance to nozzle	10 mm
Impact angle	50°

dard manner and by pressureless sintering (Thermal Technology, 1000-4560-FP2000 model furnace). Post sintering heat treatment was performed at 1900℃ for 3 hours under 0.1 MPa nitrogen gas. Flow chart of the manufacturing process is given in **Fig. 1**.

$\alpha:\beta$ phase ratio and phase composition of the intergranular phase were determined by X-ray diffraction (Rigaku 2000 Rint, Japan). Polished surfaces of the sintered samples were gold coated prior to examination in a Zeiss VP50-Supra type scanning electron microscope (SEM) by using back-scattered electron imaging mode. Analytical TEM investigations were achieved by using 200 kV field emission TEM (JEOL JEM-2100F).

Hardness and fracture toughness measurements were carried out by Vickers indentation technique by applying 10 kg load for 10 seconds. At least 5 indentations were made for each sample. The sand blast wear tests were further performed at Röchling Leripa GmbH (Austria). The test conditions were given in **Table 1**. The erosion rates of the nozzles are defined as the nozzle mass loss divided by the nozzle density and so volume of the erodent abrasive particles (wear volume) is found.

3. Results and Discussion

3.1 Powder processing challenges and solutions

Widespread use of SiAlON parts is limited at present due to high cost of raw materials and of processing. In order to solve this problem, low cost refractory grade, coarse, impure and less sinter active β-Si_3N_4 powder was used. Utilization of this kind of powder brings about processing challenges to produce SiAlON ceramics with sufficient densification, phase assemblage and mechanical properties.

The first step was before milling, characterisation of as-received β-Si_3N_4 powder. XRD analysis was carried out to detect impurities in as-received β-Si_3N_4 powder (**Fig. 2**). According to **Fig. 2**, the powder

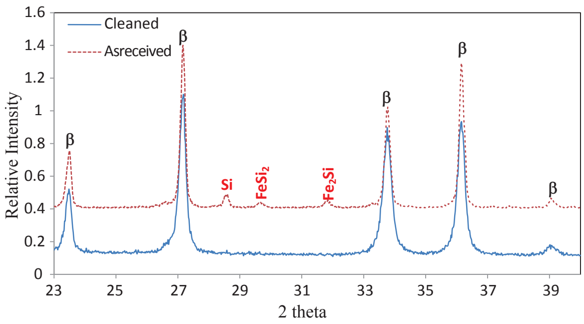

Fig. 2 An XRD analysis of cleaned and as-received β-Si_3N_4 powders.

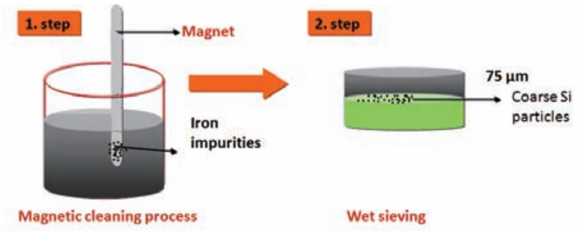

Fig. 3 Schematic illustration of iron and silicon removing processes.

contains Fe, Si, Fe_2Si and $FeSi_2$ as impurities. Iron contamination was believed to cause from the milling process of starting Si powder involving use of steel grinding media.

In order to remove iron, magnetic cleaning process was applied as shown in **Fig. 3**. Initial β-Si_3N_4 powder was mixed in mixer with isopropyl alcohol and Fe impurities were collected with a magnet. This process was repeated until iron impurities were totally removed. To remove silicon impurities, obtained slurry after magnetic cleaning process were passed under 75 µm sieves to separate coarser silicon particles. Subsequently slurry was dried in rotary evaporator. A phase comprises of as-received and cleaned β-Si_3N_4 powder is given in **Fig. 2**. XRD analysis showed that this cleaning process is effective, since there were no silicon or iron/iron containing impurities detected.

3.2 Effect of milling on powder characteristics

Initial average particle size of β-Si_3N_4 powder was measured as 10 µm by laser diffractometer (**Fig. 4**). Attrition milling in water with Si_3N_4 balls (3 mm in diameter) at 1400 rpm was performed to decrease the average particle size of β-Si_3N_4 starting powder to 1µm, 0.8 µm and 0.5 µm. The related powders were designated as B1 (d50: 1 µm), B0.8 (d50: 0.8 µm) and B0.5 (d50: 0.5 µm). For the milling process,

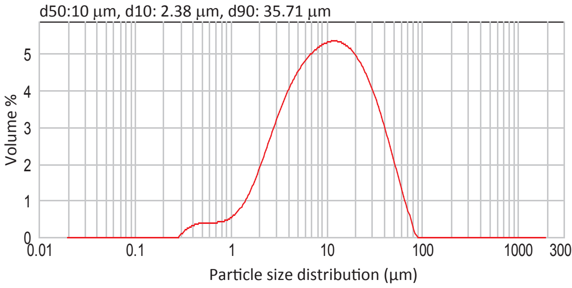

Fig. 4 Particle size distribution of as-received β-Si_3N_4 powder.

Table 2 Milling time versus particle sizes

Milling Time (h)	d50	d10	d90
0	10.05	2.38	35.71
1.5	3.58	0.89	9.34
2.5	2.59	0.84	5.79
4.5	1.40	0.55	3.22
7	1.19	0.56	2.43
9	**1.08**	0.55	2.07
11	0.98	0.46	1.97
13	**0.78**	0.30	1.69
15	0.67	0.19	1.64
17	0.62	0.20	1.50
19	0.59	0.19	1.48
21	**0.53**	0.18	1.40

Attrition milling at 1400 rpm in water

Table 3 Starting Si_3N_4 powder characteristics

	B	B1	***B0.8***	B0.5
% α-Si_3N_4	0	0	0	0
% β-Si_3N_4	100	100	100	100
D50 (µm)	10	1.08	0.78	0.53
D10 (µm)	2.4	0.55	0.30	0.18
D90 (µm)	36	2.43	1.69	1.40
Milling time (h)	-	9	13	21
Particle shape	Prismatic	Irregular	Irregular	Irregular

Table 4 XRF analyses of B0.5 powder

	N	**Si**	**Al**	**Fe**	**Ca**	**Mn**	**P**	**Sr**	**Cu**	**Ni**	**Cr**
wt%	78.97	20.38	0.450	0.0898	0.0849	0.0077	0.0030	0.0022	0.0020	0.0020	0.0019

the ratio of powder to deionised water and dispersant was 800 g : 400 g : 16 g; the weight ratio of powder to Si_3N_4 milling balls was 1: 2.3. The vessel was cooled by water circulation throughout the process. The slurry temperature was systematically controlled every hour. If slurry temperature reaches 50℃, milling speed was decreased for the duration of the next 30 minutes. Milling efficiency was given in **Table 2**. In the first 1.5 hrs, particle size was down to 3.58 µm. After 7 hrs milling, particle size was down to 1.2 µm.

SEM analysis of as-received and milled β-Si_3N_4 powder was given elsewhere[21]. As-received β-Si_3N_4 starting powder exhibited prismatic-elongated particle morphology, whereas the milled β-Si_3N_4 particles (B1, B0.8, and B0.5) showed an irregular morphology with sharp edges. The sum of initial Si_3N_4 powder characteristics were given in **Table 3**.

Total oxygen content of the powders was determined by the inert-gas-fusion method, using an elemental analyser. As-received β-Si_3N_4 powder contains 3 wt% oxygen. After 21 hours milling in water B0.5 powder has 7.8 wt% oxygen. This can be attributed to the hydrolysis of β-Si_3N_4 powder during milling in water after long hours. After 21 hours milling the slurry began to bubble with an ammonia odour. It was shown that the long term milling in isopropyl alcohol might have increased in the amount of Si-O-Si surface groups[10].

XRF analysis of B0.5 powder is given in **Table 4**. Fe, Ca, Mn, P, Sr, Cu, Ni and Cr are still present in very small quantities (less than 0.1 wt.%) in cleaned β-Si_3N_4 powder. XRF analyses verify the XRD analyses of cleaned β-Si_3N_4 powder. SEM-EDX elemental analyses of B0.5 powder showed the presence of Fe, Ca, Cu, Ba, S, Mn, Ti and Ni as impurities (**Fig. 5**).

3.3 Effect of milling time on SiAlON properties

3.3.1 Densification, phase assemblage and microstructure

Milling time is the most important variable that will effect final particle size, particle surface characteristics and hence densification, phase assemblage and microstructure. **Table 5** shows some characteristics of the powders (B1, B0.8 and B0.5), sintering conditions and some properties after sintering process. It was found that SiAlON obtained from B1 powder, milled for 9 h presents nearly full densification and designed $\alpha' : \beta'$ phase ratio was achieved. Increase in milling time from 9 to 13h leads to increase in oxygen content of Si_3N_4 powder and this variation causes increase in β' content. During milling in water, following reaction may occur[22].

$$Si_3N_4 + 6H_2O \rightarrow 3SiO_{2\ \mathrm{amorphous}} + 4NH_3 \qquad \text{(i)}$$

SiO_2 formation due to this reaction shifts the composition to β' rich region. It is also expected that increased silica would preferentially react with α-SiAlON stabilizing additives and thus would reduce/prevent α-SiAlON formation.

Other important topic is sintering of coarse B0.8 powder by pressureless sintering route at 1800℃, for

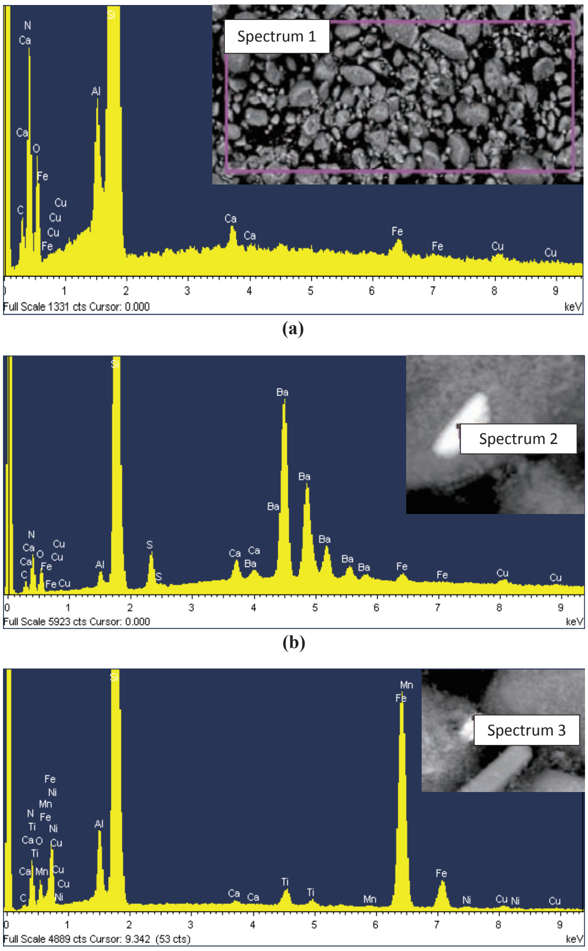

(a)

(b)

(c)

Fig. 5 SEM-EDX analyses of B0.5 powder.

1 h with almost full densification due to judiciously selection of dopant system[23]. One of the main aspects in designing SiAlONs with improved properties would be the chosen of additives that would provide a good liquid phase sintering behaviour. In this study Sm rich Y-Sm-Ca dopant system with cation molar ratio 30:64:6 was chosen because of the low eutectic temperature and high nitrogen solubility of the Sm-Si-Al-O-N system[24]. Moreover, the viscosity of Sm-Si-Al-ON liquids is less than the other lanthanide containing SiAlONs and this makes densification easier[24]. Further increase in milling time to 21 h results in further increase in oxygen content up to 7.8 wt.%. Higher oxygen content induces more liquid phase during sintering and leads to better densification even at 1850℃ but it has detrimental effect on high temperature properties due to higher liquid phase content.

Table 5 Characteristics of SiAlON ceramics

Powder	Milling Time (h)	O (wt. %)	Sintering Conditions	Phase Assemblage	Relative Density
B1	9	4	1940°C, 2 h, 2.2 MPa N_2	$73\beta':27\alpha'$	99.90
B0.8	13	4.7	1800°C, 1 h, 0.1MPa N_2 HT: 1900°C, 3 h, 0.1MPa N_2	$81\beta':19\alpha'$	99.90
B0.5	21	7.8	1850°C, 1 h, 2.2 MPa N_2	$100\beta'$	99.43

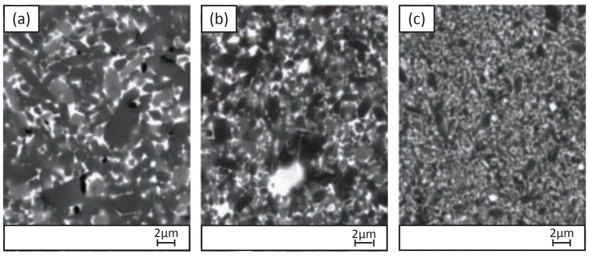

Fig. 6 BSE-SEM images of sintered SiAlONs prepared from (a) B1, (b) B0.8 and (c) B0.5 powders.

Fig. 6 shows BSE-SEM images of sintered SiAlONs prepared from β-Si_3N_4 powders which were subjected to different milling times. The differences in microstructure can be explained on the basis of differences in powder particle size and sintering conditions. The microstructure of B1 sample consisted of predominantly between 1-1.4 μm α' and β' grains diameter, the aspect ratio of grains changes between 2.5 to 7 (**Fig. 6a**). The diameter and length of grains were determined by the SEM micrographs of polished surfaces. Over 200 grains of each sample were measured. The apparent aspect ratio of the grains was calculated by dividing the length to diameter. A decrease in β-Si_3N_4 particle size to 0.8 μm (B0.8) resulted in decrease in α' and β' grains diameter to between 0.5-1.5 μm, but aspect ratio of grains almost similar (**Fig. 6b**). This sample was subjected to heat treatment at 1900℃ for 3 hrs under 0.1 MPa nitrogen gas pressure. However, substantial grain growth was not achieved due to coarse grain size of sintered samples. In order to obtain grain growth, grain size should be less than 0.5 μm. It was observed that in order to achieve grain growth and to develop self reinforced microstructure after heat treatment, the grain size of SiAlON after sintering should be rather fine, preferably less than 0.5 μm as in **Fig. 7** [21]. Otherwise, coarse grains, even around 1 μm, do not have enough driving force for grain growth. Similar observations were made on β-Si_3N_4 ceramics[25-28].

After 21 hrs milling, particle size was down to 0.5 μm and B0.5 specimen after sintering have fine elongated microstructure with grain size was around 0.2 μm and aspect ratio was about 7. It is evident that final grain size of β-Si_3N_4 derived SiAlON ceramics depends on the initial β-Si_3N_4 particle size (**Fig. 8**). During sintering, the solution of β-Si_3N_4 in the

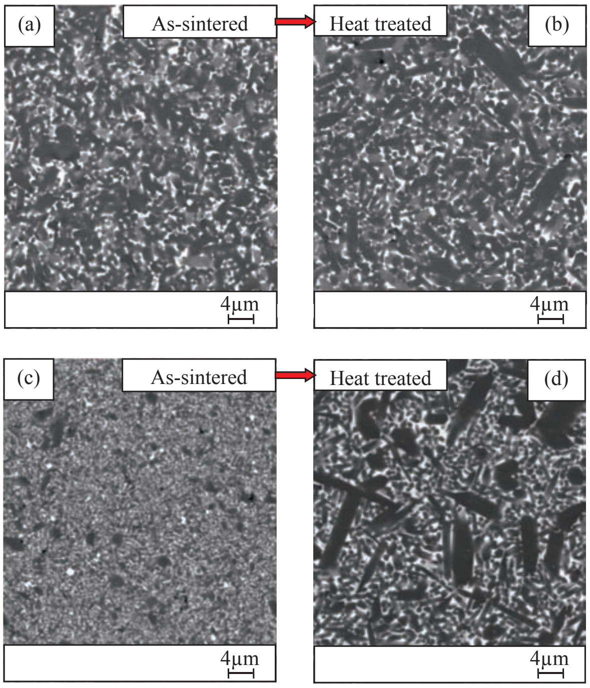

Fig. 7 BSE-SEM images representing the as-sintered and heat treated microstructure of (a, b) B1 and (c, d) B0.5.

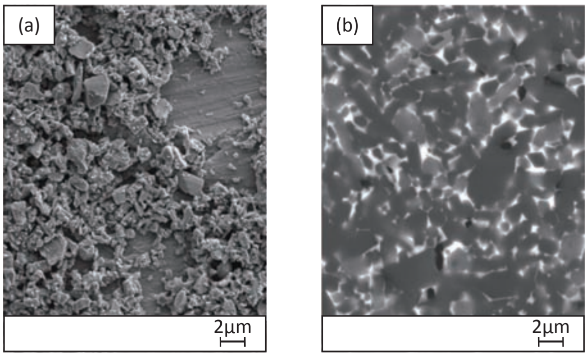

Fig. 8 (a) SEM-SE image of starting β-Si_3N_4 powder (d50:1 μm) and (b) SEM-BSE image of sintered B1 sample.

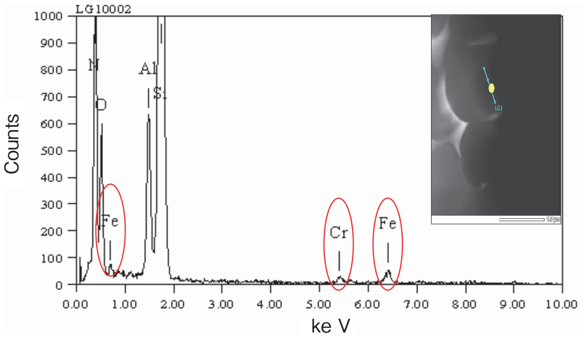

Fig. 9 TEM-EDX analyses of B1 sintered sample.

liquid phase and precipitation as $\alpha:\beta$-SiAlON might have caused the formation of $\alpha:\beta$-SiAlON from β-Si_3N_4 powder [18]. The nucleation can either be homogeneous from the liquid or heterogeneous on the existing β-Si_3N_4 grains. Given the fact that the initial particle size is an effective parameter on the final microstructure, the use of coarse or fine β-Si_3N_4 powders resulted in coarse or fine $\alpha:\beta$-SiAlON, respectively. It appears that nucleation of $\alpha:\beta$-SiAlON occurred heterogeneously on the pre-existing crystals in case of B0.8 and B1 powders.

Even if the starting β-Si_3N_4 powder was subjected to magnetic cleaning and sieving processes, some impurities may remain in powder. After a detailed TEM-EDX examination of the sintered SiAlON samples prepared from B1 powder, incorporation of undesirable Fe and Cr impurities into the β-SiAlON crystal structure was found (**Fig. 9**) [29]. As previously noted Be [30], Mg, Li [31] and Ga [32] may enter β-Si_3N_4 crystal structure. These results clearly showed that Fe and Cr can enter β-SiAlON crystal structure. As a conclusion it can be inferred that the use of Si_3N_4 powders with certain impurities can be used to produce a SiAlON phase microstructure.

3.3.2 Mechanical properties

The hardness and fracture toughness values of the SiAlON ceramics are summarized in **Table 6**. Increasing milling time resulted in a decrease in hardness. During milling in water, oxygen content of the composition increased. Therefore, the initial composition shifted to β' region. In addition, higher oxygen content led to a higher fraction of intergranular phase. This increment provided a decrease in hardness. B1 and B0.8 have similar hardness values. The difference in hardness between B1, B0.8 with that of B0.5 can be attributed to the presence of larger fraction of grain boundary phase in B0.5 due to prolonged milling time and also to the absence of harder α' phase. Although B1 and B0.8 specimens consisted of both α' and β' phases, hardness values were lower than expected. As mentioned before, incorporation of Fe and Cr impurities in β' crystal structure might have caused a decrease in hardness values.

Both indent diagonals and crack lengths around the indentations were measured from the SEM images and found that l/a ratio varies between 1.0 and 1.7 and such values indicated good crack growth resistance property of the investigated ceramics. The differences in microstructure and properties can be explained on the basis of differences in powder particle size. The development of more elongated grains

Table 6 Mechanical properties and developed phases of SiAlONs, prepared from different starting particle sizes 1 µm (B1), 0.8 µm (B0.8) and 0.5 µm (B0.5), when subjected to different sintering methods and heat treatment

Sample	Milling time (h)	HV (GPa)	Kıc (MPam$^{1/2}$)	Phases
B1	9	14.22 ± 0.03	5.30 ± 0.15	73 β':27 α'
B0.8 (HT)	13	14.10 ± 0.07	5.20 ± 0.10	81 β':19 α'
B0.5	21	13.00 ± 0.03	5.60 ± 0.20	100 β'

in B0.5 resulted in relatively higher toughness than other sintered ceramics. B1 and B0.8 samples have similar aspect ratio (see **Fig. 6**) and thus fracture toughness values are similar. Post sintering heat treatment did not have any effect on grain growth for B0.8 sample (**Fig. 7**). It was concluded that to achieve grain growth and to develop self-reinforced microstructures by heat treatment, grain size of SiAlON microstructure after sintering should be less than µm (preferably ≤ 0.5 µm). Coarse grains would not have enough driving force for grain growth.

3.3.3 Wear resistance

Table 7 presents the hardness, flexural strength, fracture toughness, phase assemblage and wear volume of the samples. Sand blast wear tests were carried out on the developed SiAlON ceramics to simulate wear caused by severe particle impacts. In addition the wear volume of the developed cost effective SiAlON was compared with commercial ceramic materials were provided from CeramtecAG company (Germany) which are commonly used in wear applications.

The sand blast test results showed that SiAlON ceramic was much more durable than alumina ceramics which are widely used in wear applications. Although commercial Al_2O_3-ZrO_2 material is harder than B0.8 monolithic SiAlON, B0.8 monolithic SiAlON is 4.5 times more durable than commercial Al_2O_3-ZrO_2 material. SiAlON showed similar performance to silicon nitride ceramics although it was prepared from cost effective heterogeneous powders. When the hardness, toughness and strength values are compared, commercial Si_3N_4 proved advantageous over B0.8 sample. However, wear volume values are almost similar. In general, it can be concluded that SiAlON ceramics have better properties than Si_3N_4 ceramics for commercial applications.

Table 7 Properties and wear volumes of sand blast tested ceramics

Sample	HV (GPa)	K_{IC} (MPam$^{1/2}$)	Strength (MPa)	Phases	Wear Volume (mm^3)
B0.8	14.10	5.1	530	81 β':19 α'	0.0360
Commercial Si_3N_4	16.00	5.5	850	β - Si_3N_4	0.0320
Commercial Al_2O_3-ZrO_2	17.00	4.4	450	Al_2O_3-ZrO_2	0.1600
Commercial Al_2O_3	17.00	4.0	380	Al_2O_3	0.4800

4. Conclusions

In this article, processing challenges of β-Si_3N_4 powder to produce SiAlON ceramics have been tried to clarify. It has been found that undesired iron and silicon impurities in starting silicon nitride powder can be significantly reduced by magnet and then wet sieving. On the other hand, incorporation of undesirable impurities into the β-SiAlON crystal structure and thus use of Si_3N_4 powders with certain impurities as characterized by TEM, are found to be possible.

The effect of powder processing conditions on phase assemblage, densification, microstructure and mechanical properties of SiAlON parts has been identified. The powder milling time was determined to see the effects on creating silica on silicon nitride powder. Silica content on silicon nitride powder governed the phase assemblage. If oxygen content is ~7.8 wt%, the designed α':β' ratio was not achieved and composition was shifted to β' rich region. It was observed that initial particle size have vital effects on microstructural evolution. If particle size is larger than 0.5 µm low aspect ratio grains developed. A combination of hardness of around 14 GPa and indentation toughness of 5.1 MPam1/2 could be obtained in ceramics sintered from coarse (0.8 µm) β-Si_3N_4 powders. This SiAlON ceramics prepared by with commercial Si_3N_4, showed similar wear resistance performance and proved more durable than commercial alumina ceramics which are widely used in wear applications.

Acknowledgement

The authors specially thank Prof.Dr. Ferhat Kara and Dr. Hilmi Yurdakul from Anadolu University for valuable discussion on the processing and TEM observations respectively. In addition, the financial support of the Scientific and Technological Research Council of Turkey (TUBITAK) (Ankara, Turkey) and the Ministry of Science, Industry and Technology under the framework of the San-Tez Programme have been gratefully acknowledged.

References

1) Ekström, T. and Nygren, M. (1992) : SiAlON ceramics, J. Am Ceram Soc, Vol.75, pp.259-276.
2) Mitomo, M. and Tayima, Y. (1991) : Sintering, properties and applications of silicon nitride and SiAlON ceramics, J. Jpn. Ceram. Soc., Vol.99, pp.1014.
3) Riley, F. (2000): Silicon nitride and related materials, J. Am. Ceram. Soc., No.83, pp.245-265.
4) Li, H. X., Sun, W. Y., Wang, P. L., Yan, D. S. and Tien, T. Y. (1997) : The effect of GPS parameters on mechanical properties of Y-α-SiAlON ceramics, Ceramics International, Vol.23, pp.449-56.
5) Hayama, S., Nasu, T., Ozawa, M. and Suzuki, S. (1997) :Mechanical properties and microstructure of reaction sintered β′-sialon ceramics prepared by a slip casting method, Journal of Materials Science, Vol.32, pp.4973-4977.
6) Salamon, D., Šajgalík, P., Liška, M. (2005) :Mechanical Properties and Microstructure of α-SiAlON Based Cutting Tools, Key Engineering Materials, Vol.290, pp.250-253.
7) Kumar, R., Acikbas Calis, N., Kara, F., Mandal, H., and Basu, B, (2009) : Microstructure - Mechanical Properties - Wear Resistance Relationship of SiAlON Ceramics, Metallurgical and Materials Transactions A, Vol.40, pp.2319-2332.
8) Rabe, T., and Linke’ D. (1992) : Attrition milling of silicon nitride powder under conditions for minimal impurity pickup, Ceramics International, Vol.18, pp.161-166.
9) Dai, J. Q., Huang, Y., and Ma, J. T. (2008) : Surface characteristics and aqueous dispersibility of commercial silicon nitride powders : Effects of acid leaching, surface hydrolysis and thermal oxidation, Ceramics International, Vol.34, pp.1835-1842.
10) Huang, Y., Dai, J. Q., Xie, Z. P., Ma, T., Yang, J. L., Ma, J. T. (2003) : Effects of liquid medium and ball milling on the surface group and aqueous dispersibility of Si_3N_4 powder, J. Euro. Ceram. Soc., Vol.23, pp.985-990.
11) Tapaszto, O. and Balazsi, C. (2010) :The efeect of milling time on the sintering kinetics of Si_3N_4 based nanocomposites, Ceramics International, Vol 36, pp.2247-2251.
12) Naito, M., Okumiya, M., Abe, H., Kondo, A., Huang, C.C. (2010) : Powder processing issues for high quality advanced ceramics, KONA Powder and Particle Journal, N0.28, pp.143-154.
13) Acikbas Calis, N., Kara, F., Mandal, H. (2009) :Development of α-β SiAlON Ceramics From Different Si_3N_4 Starting Powders, Key Engineering Materials, Vol.403, pp.107-108.
14) Herrmann, M., Höhn, S., Bales, A. (2011) : Kinetics of rare earth incorporation and its role in densification and microstructure formation of alpha-Sialon, J. Euro. Ceram. Soc., Vol.32, pp.1313-1319.
15) Rhee, S. H., Lee, J. D and Kim, D. Y. (2000): Effect of α-Si_3N_4 initial particle size on the microstructural evolution and phase transformation during sintering of Si_3N_4 ceramics, J. Euro. Ceram. Soc., Vol.20, pp.1787-1794.
16) Lee, C. J., Chae, J. I. and Kim, D. J., (2000): Effect of β-Si_3N_4 starting powder size on elongated grain growth in β-Si_3N_4 ceramics, J. Euro. Ceram. Soc., Vol.20, pp.2667-2671.
17) Mitomo, M. and Uenosono, S. (1992) : Microstructural development during gas-pressure sintering of α-silicon nitride, J. Am. Ceram. Soc., Vol.75, pp.103-107.
18) Ekström, T., Ingelström, N., Brage, R., Hatcher, M. and Johansson, T. (1988): α-β-SiAlON ceramics made from different silicon nitride powders, J. Am. Ceram. Soc., Vol.71, pp.1164-1170.
19) Li, Y. W., Wang, P. L., Chen, W. W., Cheng, Y.B. and Yan, D.S. (2000) : Phase formation and microstructural evolution of Ca α-SiAlON using different Si_3N_4 starting powders, J. Euro. Ceram. Soc., Vol.20, pp.1803-1808.
20) Irene G. Cano and Miguel A. Rodríguez (2004) : Synthesis of β-Silicon nitride by SHS: fiber growth, Scripta Materialia, Vol.50, pp.383-386.
21) Acikbas Calis, N., Kumar, R., Kara, F., Mandal, H., and Basu, B (2011): Influence of β-Si_3N_4 particle size and heat treatment on microstructural evolution of α : β-SiAlON Ceramics, J. Euro. Ceram. Soc., Vol.31, pp.629-635.
22) Boris, E. L., Zhmud, V. and Bergstrom, L. (2000) : Dissolution and Deagglomeration of Silicon Nitride in Aqueous Medium, J. Am. Ceram. Soc., Vol.83, pp.2394-2400.
23) Kara, F., Mandal, H., Turan, S., Kara, A. and Acikbas Calis, N.: Development Strategies for SiAlON Ceramics, Global Roadmap for Ceramics ICC2 Proceedings, pp.119-128, 2nd International Congress on Ceramics, June 29-July 4, Verona, Italy, 2008.
24) Mandal, H. (1992): “Heat treatment of sialon ceramics”, PhD. Thesis, University of Newcastle Upon Tyne, 149pp.
25) Mitomo, M., Tsutsumi, H., Tanaka, S., Uenosono, S. and Saito, F. (1990): Grain growth during gas-pressure sintering of β-silicon nitride, J. Am. Ceram. Soc., Vol.73, pp.2441-2445.
26) Lee, C. J., Chae, J. I. and Kim, D. J. (2000): Effect of beta-Si_3N_4 starting powder size on elongated grain growth in bet]-Si_3N_4 ceramics, J. Eur. Ceram. Soc., Vol.20, pp.2667-2671.
27) Mitomo, M., Hirotsuru, H., Suematsu, H. and Nishimura, T. (1995): Fine-grained silicon nitride ceramics prepared from β-powder, J. Am. Ceram. Soc., Vol.78, pp.211-214.
28) Hirosaki, N., Akimune, Y. and Mitomo, M. (1993): Effect of grain growth of β-silicon nitride on strength, Weibull modulus, and fracture toughness, J. Am. Ceram. Soc., Vol.76, pp.1892-1894.
29) Yurdakul, H., and Turan, S. (2011): Incorporation of the transition metals (Cr and Fe) into beta-SiAlON crystal structure, Ceramics International, Vol.37,

pp.1501-1505.
30) Huseby, I.C., Lukas, H.L. and Petzow, G., (1975) :Phase equilibria in the system Si_3N_4-SiO_2-BeO-Be_3N_2, J. Am. Ceram. Soc., Vol.58, pp.378-380.
31) Jack, K.H. (1973) :Nitrogen Ceramics, Trans, J. Br.Ceram. Soc., Vol.72, pp.376-384.
32) Oyama, Y. (1973) :Solid Solution in the System Si_3N_4-Ga_2O_3-Al_2O_3, Jpn. J. Appl., Phys., Vol.12, pp.500-508.

Author's short biography

Hasan Mandal

Hasan Mandal (Prof. Dr.) received his PhD in Ceramic Materials from University of Newcastle (UK) in 1992. In the period of 2007-2008, Dr. Mandal was at Karlsruhe University as Alexander von Humboldt Fellow. In 1996, he joined the Department of Ceramic Engineering at Anadolu University. He became the Head of Department (1999), Dean of the Faculty of Engineering (2004), Chairperson of Turkish Engineering Deans Council (2006), Chairperson of Global Engineering Deans Council (GEDC-2009), Vice Rector of Anadolu University (2010). He is currently is Vice President and also the Director of Research and Graduate Policies at Sabanci University/Istanbul. He has co-authored over a hundred publications, three patents about science and technologies on Si3N4 based ceramics including phase relationships, structure-property relations and applications. Because of these achievements, he was honoured by twenty awards including European Ceramic Society, Stuijts Award in 2005. He is a member of World Innovation Foundation and World Academy of Ceramics.

Nurcan Calis Acikbas

Nurcan Calis Acikbas received B.S., M.S. and PhD. Degrees in Ceramic Engineering from Anadolu University, Turkey in 2002, 2004 and 2009, respectively. She was with MDA Advanced Ceramics Ltd. from 2004 to 2010. She joined the Bilecik University, Mechanical and Manufacturing Engineering Department as assistant professor. She appointed as Deputy Director of Bilecik University Central Research Laboratory at 2011. She was honoured by award Turkey Technology Development Foundation (TTGV) the most successful thesis in university-industry collaboration. Her current research interest is structure-property relationship; tribology; Silicon Nitride based ceramics and its applications.